Inorganic Chemistry

Article

pubs.acs.org/IC

Multifunctional Zn(II) Complexes: Photophysical Properties and Catalytic Transesterification toward Biodiesel Synthesis

Abhishek Kumar Gupta, Abhimanew Dhir, and Chullikkattil P. Pradeep*

School of Basic Sciences, Indian Institute of Technology Mandi, Kamand 175 005, Himachal Pradesh, India

Supporting Information

ABSTRACT: Using 4-substituted derivatives of phenol-based compartmental Schiff-base hydroxyl-rich ligand, four multifunctional binuclear Zn(II) complexes have been synthesized and characterized. The photophysical properties of these complexes were explored in the solid state, in solutions, and in poly(methyl methacrylate) (PMMA) matrix, which revealed their good potential as tunable solid state emitters. Some of these complexes acted as efficient catalysts for the transesterification of esters and canola oil showing their potential in biodiesel generation. Mechanistic investigations using ESI-MS revealed that the transesterification catalyzed by these complexes proceeds through two types of acyl intermediates.

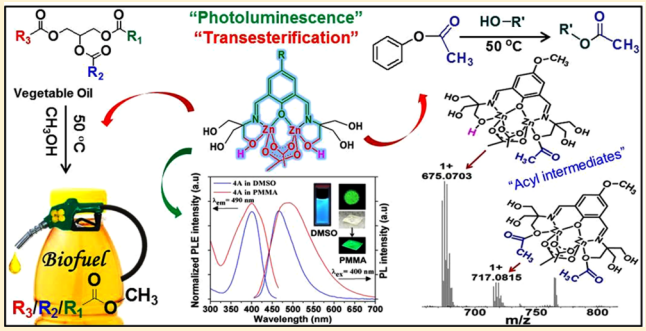

INTRODUCTION

Development of novel multifunctional transition metal complexes and materials is gaining interest among researchers working in diverse areas. Transition metal complex based "theranostics" which combine therapy and diagnostic imaging into a single modality are good examples of such multifunctional systems.[1] Many materials useful for multiple applications have also been developed in recent years.[2] On the molecular level, judicious selection of ligand and metal cation permits the assembly of multicomponent molecular systems capable of performing varied functions inaccessible for a simple molecule system.[3] This is because the properties of a coordination compound are often more than the simple sum of the properties of the ligand and metal ion. However, the rational design of a ligand system that permits different parts of a coordination complex to perform different functions is still a challenging task.

In this regard, we were interested in developing novel transition metal complexes for multiple applications like photoluminescence and catalysis. Toward this, we have developed a series of compartmental Schiff base hydroxyl-rich ligands (hrls) from substituted 2,6-diformyl phenols and tris(hydroxymethyl)aminomethane (tris). Compartmental Schiff base ligands, especially those based on 2,6-diformyl phenol, are known to function as versatile tectons in designing luminescent materials.[4] Ligands with tripodal alcoholic arms as present in tris can ensure versatile chelating and bridging platforms through alcoholic or alkoxide coordination that can support high oxidation states of metal ions as well.[5] In the present study, we selected Zn(II) as metal ion due to its high Lewis acidity, which is desirable for certain catalysis applications such as transesterification.[6] Biologically, Zn(II)-bound alkoxides, derived from the deprotonation of Zn(II)-bound internal alcoholic residues (e.g.: serine, threonine) in Zn(II)-containing enzymes, are known to act as strong nucleophiles to attack electrophilic substrates leading to reactions like ester hydrolysis and transesterification.[7] Moreover, Zn complexes of functional organic ligands are known to exhibit photoluminescent properties and have found applications in light emitting diodes.[8] There are a few recent reports on multifunctional materials exhibiting photophysical and catalytic properties in the literature.[2]

We report herein a series of binuclear Zn(II) complexes **4A**–**4D** having the general formula $[Zn_2(R\text{-dfp})(O_2CMe)_2]\cdot(O_2CMe)\cdot nH_2O$ (R = −OMe, n = 2 (**4A**); R = −Me, n = 2 (**4B**); R = −COOEt, n = 3 (**4C**); R = −Br, n = 1 (**4D**)) (where dfp = 2,6-bis((*E*)-(1,3-dihydroxy-2-(hydroxymethyl)propan-2-ylimino)methyl)phenol with deprotonated phenolic group and R-dfp is 4-substituted dfp). All of these complexes have at least two distinct structural subunits: an upper aromatic diimine chromophoric unit and lower Zn-alcoholic OH units as shown in Figure 1.

We reasoned that these two distinct structural subunits may be exploited separately for different applications like photoluminescence and catalytic transesterification including biodiesel synthesis.[9] Mechanistic aspects of the transesterification reactions catalyzed by complexes **4A**–**4D** have been explored using ESI-MS analyses.

EXPERIMENTAL SECTION

Materials and Methods. All reagents were purchased from Sigma-Aldrich or TCI and were used without further purification. Synthetic procedures of ligands **3A** and **3C** and complex **4B** have been

Received: March 31, 2016

DOI: 10.1021/acs.inorgchem.6b00804
Inorg. Chem. XXXX, XXX, XXX−XXX

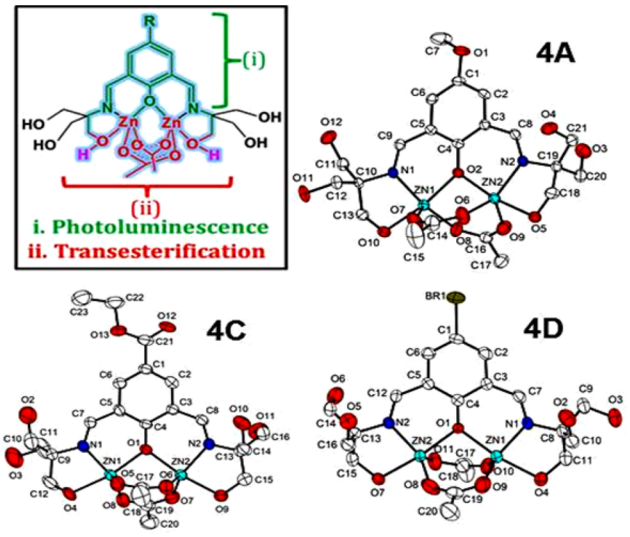

Figure 1. ORTEP diagrams (50% probability level) of complexes **4A**, **4C**, and **4D** with atom-numbering scheme. H atoms, uncoordinated CH_3COO^-, and solvent molecules are omitted for clarity. Color code: Zn, cyan; N, blue; O, red; C, white; Br, yellow. Inset: Schematic representation of complexes **4A**–**4D** highlighting different parts responsible for different functions.

reported earlier.[10,5b] FT-IR spectra were measured on Agilent Cary-660 FT-IR spectrometer with solid samples using a Diamond ATR accessory. ^{1}H and ^{13}C NMR spectra were recorded on Jeol JNM ECX-500 FT-NMR spectrometer using D_2O, DMSO-d_6, and CD_3OD as solvents and TMS as internal standard. NMR data are reported as follows: chemical shift in ppm (δ), multiplicity (s = singlet, d = doublet, br = broad singlet, m = multiplet), coupling constant J (Hz), integration, and interpretation. ESI-TOF HR-MS spectra were recorded on Bruker Maxis Impact instrument. Elemental analyses were performed on a varioMICRO CHNS instrument. Canola oil (CO) (Jivo brand, Canada) was purchased from a local grocery store and used without further puification. CO contains 7.5% of saturated fat (C18:0), 62.0% of monounsaturated fat (C18:1), 30.1% of polyunsaturated fat (C18:2 ca. 21.0% and C18:3 ca. 9.1%), and 0.4% of trans fat.

Photoluminescence (PL), Lifetime, Quantum Yield, and Electrochemical Measurements. Photoluminescence (PL) spectra were measured by using a Fluorolog-3 spectrofluorometer (Horiba-Jobin-Yvon). Spectra were corrected for variations in excitation intensity and response of the detector. The concentrations of Zn complexes in dimethyl sulfoxide (DMSO) and poly(methyl methacrylate) (PMMA) matrix were chosen so as to give an absorbance less than 0.1 at the excitation wavelength. UV–vis spectra were recorded on a Shimadzu UV-2450 spectrophotometer. The fluorescence lifetimes were measured using a Horiba scientific Delta Flex TCSPC system with Pulsed LED sources excited at 390 nm. Ludox was used as an IRF for deconvolution of the spectral values.

Total PL quantum yields (PLQY) (at an ambient temperature of 295 K), were determined by absolute measurements using a quanta-φ F-3029 sample chamber of the Fluorolog spectrometer having an integrating sphere of diameter 15.2 cm coated with Spectralon material (reflectivity >95% from 250 to 2500 nm). Samples were inserted into the sphere and excited with wavelengths 360–400 nm, depending on the complexes' excitation wavelength. PLQYs were referenced to that of quinine sulfate (QS) excited at 350 nm dissolved in 0.05 M H_2SO_4, according to a reported procedure.[11] The PLQY of QS was taken as 0.60. The accuracy of the determination of PLQY was estimated to be ±10%.

All electrochemical measurements were carried out on a Metrohm Autolab instrument using 5×10^{-3} M solutions of samples in DMSO containing 0.1 M tetrabutylammonium hexafluorophosphate (Bu_4NPF_6) as electrolyte. Glassy carbon electrode was used as working electrode, Ag/AgCl as reference electrode, and platinum wire as counter electrode. Solutions were purged with argon prior to each experiment, and the scans were performed at a rate of 100 mV s^{-1} at room temperature. The values of the potentials quoted in this work are given with respect to the Fc/Fc^+ redox couple. The energy level of Fc/Fc^+ was assumed at −4.8 eV to vacuum.[12] The LUMO energy levels of the complexes were calculated using the equation $E_{LUMO} = -(4.8 - E_{1/2,Fc/Fc^+} + E_{red,onset})$, where $E_{red,onset}$ is the onset reduction potential.

Table 1. Crystal and Structure Refinement Data for Complexes 4A, 4C, and 4D

compound	4A	4C	4D
empirical formula	$C_{23}H_{38}N_2O_{16}Zn_2$	$C_{50}H_{84}N_4O_{36}Zn_4$	$C_{22}H_{33}BrN_2O_{14}Zn_2$
formula wt	729.29	1578.69	760.15
cryst syst	triclinic	monoclinic	triclinic
space group	$P\bar{1}$	$P2_1/c$	$P\bar{1}$
a/Å	9.4617(6)	16.0116(7)	9.5367(8)
b/Å	12.8137(8)	29.3742(10)	12.0547(10)
c/Å	12.9974(8)	14.5726(6)	13.1566(11)
α/deg	82.901(5)	90	97.977(7)
β/deg	85.705(5)	105.562(5)	94.890(7)
γ/deg	76.749(5)	90	112.142(8)
U/Å^3	1520.31(17)	6602.6(5)	1371.7 (2)
Z	2	4	2
D_c/Mg m^{-3}	1.593	1.588	1.697
μ/mm^{-1}	1.653	1.534	3.266
F(000)	756	3280	710
cryst size (mm^3)	0.2604 × 0.1418× 0.1111	0.367 × 0.33 × 0.2283	0.2074 × 0.1257 × 0.0992
T/K	293(2)	293(2)	293 (2)
reflns collected/unique	8535/6554 [R(int) = 0.0213]	22971/13939 [R(int) = 0.0320]	6997/5481[R(int) = 0.0920]
data/restraints/params	6554/0/414	13939/6/873	5478/2/347
R1,[a] wR$_2$[b] [$I > 2\theta(I)$]	0.0398, 0.1002	0.0737, 0.1640	0.0459, 0.1164
R$_1$,[a] wR$_2$[b] (all data)	0.0502, 0.1076	0.1296, 0.2082	0.0820, 0.1442
GOF	1.050	1.066	0.955

[a]R1 = $F_o - F_c/F_o$. [b]wR2 = $[w(F_o^2 - F_c^2)^2/w(F_o)^2]^{1/2}$.

DOI: 10.1021/acs.inorgchem.6b00804
Inorg. Chem. XXXX, XXX, XXX–XXX

The HOMO energy levels of complexes were calculated by subtracting the optical band gap value ($E_{g,opt}$) from the respective LUMO energy levels ($E_{HOMO} = E_{LUMO} - E_{g,opt}$).[13] The optical band gaps were determined from the intersection of absorption and emission spectra.[14]

Gas Choromatography (GC) Analyses. Gas chromatograms were recorded on an Agilent 7890A series gas chromatograph system equipped with HP-5/DB-wax columns. Flame ionization detector (FID) and N_2 carrier gas were used for sample analyses. Agilent open lab control panel software A.01.05 (1.3.19.115) was used to analyze the results and to operate the GC system.

X-ray Crystallographic Studies on 4A, 4C, and 4D. Single crystal X-ray diffraction data were collected on an Agilent SuperNova diffractometer, equipped with dual source (Cu and Mo) and Eos CCD detector, using Cu Kα radiation (1.54184 Å) at 293 K. Data acquisition, reduction, and absorption correction were performed by using CrysAlisPRO program.[15] The structures were solved by direct methods with ShelXS[16] and refined on F^2 by full matrix least-squares techniques with ShelXL[16] using the Olex[2] (v.1.2) program package.[17] Anisotropic displacement parameters were applied for all atoms, except hydrogen atoms and some solvent molecules and counterions. H atoms were calculated into their respective positions or were located from the electron density map and refined as riding atoms using isotropic displacement parameters.

The counterion present in the structure of **4D** was highly disordered, so the SQUEEZE procedure of PLATON program[18] was applied, which suggested 38 electrons per unit cell. One acetate ion contains 32 electrons. Therefore, the 38 electrons suggested by SQUEEZE is close to the electron density required for one acetate ion. The contents of the unit cell are presented accordingly.

In general, the crystals of complexes **4A**, **4C**, and **4D** were weakly diffracting and therefore the quality of data were relatively poor. As a result of this, the probability of finding less intensely scattered atoms like hydrogen was less, especially for those on the solvent molecules. Therefore, we fixed the hydrogen atoms manually in most of the cases, except a few, based upon their geometrically calculated positions. Because of the problems associated with the location of hydrogens in their exact position, Checkcif alerts of "short inter D−H···H−D contacts", "D−H without acceptor", etc. were generated for all the crystals. Most of these alerts were about the location of hydrogens on solvent water molecules. However, the connectivity around such solvent molecules is well-defined, and therefore, there is little doubt on the average location of such H atoms.

Again, due to the poor quality of diffraction data and small unresolved disorders exhibited by certain solvent molecules, counterions, etc., alerts like high "ADP max/min ratio", "high 'MainMol' Ueq as compared to neighbors", etc. were generated for **4C**. In addition, ADDSYM detected a new (pseudo) symmetry element as well for this crystal, but our attempts to solve and refine the structure in the suggested space group were unsuccessful.

The crystal and structure refinement data are summarized in Table 1, and selected bond lengths and bond angles are given in Table S1. Crystallographic data are available as Supporting Information for 4A, 4C, and 4D. In addition, CCDC 1470566 (**4A**), 1470567 (**4C**), and 1470568 (**4D**) contain the supplementary crystallographic data for this paper. These data can be obtained free of charge from The Cambridge Crystallographic Data Centre via www.ccdc.cam.ac.uk/data_request/cifdata.

*Synthesis of Ligand **3D**.* A dry methanolic solution (30 mL) of 5-bromo-2-hydroxybenzene-1,3-dialdehyde[19] (1.00 g, 4.36 mmol) was heated for 10 min at 50 °C. After getting a clear yellow solution, tris(hydroxymethyl)aminomethane (tris) (1.06 g, 8.73 mmol) was added to it and the resulting solution was heated under reflux for 6 h under dry conditions. After solvent evaporation, an orange colored gummy product was obtained. The product was washed sequentially with ethyl acetate and diethyl ether and dried under vacuum to get **3D**. Yield: 1.50 g (79%). IR (ATR, cm^{-1}): 3286 (O−H), 2874 (C−H), 1680 (C═N). ^1H NMR (500 MHz, CD_3OD): δ = 8.54 (s, 2H, HC═N), 7.49 (s, 2H, Ar−H), 5.62 (s, 1H, Ar−OH), 3.82 (s, 12H, CH_2) ppm. ^{13}C NMR (100 MHz, CD_3OD): δ = 167.9, 165.76, 136.59, 132.64, 119.55, 64.04, 56.06 ppm. ESI-MS: m/z 437.07 $[\mathbf{3D} + H]^+$.

*Synthesis of Complex **4A**, $[Zn_2(OMe\text{-}dfp)\ (OAc)_2](OAc)\cdot 2H_2O$.* A solution of $Zn(OAc)_2\cdot 2H_2O$ (0.11 g, 0.52 mmol) in 5 mL of dry methanol was added into 15 mL of a methanolic solution of **3A** (0.10 g, 0.26 mmol) followed by the addition of triethylamine (TEA) (0.07 mL, 0.52 mmol), and the reaction mixture was stirred at room temperature for 6 h. After this, the solvent was removed and the residue obtained was washed with diethyl ether and dried. This product was dissolved in methanol−chloroform (1:2, v/v) solvent mixture and kept for crystallization by slow evaporation method at room temperature. After 2 days, orange block crystals were isolated. Yield: 0.12 g (73%). ESI-MS: m/z = 633.05 $[C_{21}H_{31}N_2O_{12}Zn_2]^+$ (calcd m/z = 633.04). Anal. Calcd for $C_{23}H_{38}N_2O_{16}Zn_2$: C, 37.88; H, 5.25; N, 3.84. Found: C, 37.98; H, 5.77; N, 4.11. IR (ATR, cm^{-1}): 3217 (O−H), 2930 (C−H), 1630(C═N), 1553 (OCH_3).

*Synthesis of Complex **4B**, $[Zn_2(CH_3\text{-}dfp)\ (OAc)_2](OAc)\cdot 2H_2O$.* A binuclear zinc complex of ligand **3B** has already been reported earlier.[5b] For our studies, we synthesized complex **4B** using a synthetic procedure same to that used for complex **4A**. ESI-MS: m/z 617.03 $[C_{21}H_{31}N_2O_{11}Zn_2]^+$ (calcd 617.04). Anal. Calcd for $C_{23}H_{38}N_2O_{15}Zn_2$: C, 38.73; H, 5.37; N, 3.93. Found: C, 38.58; H, 5.18; N, 4.02.

*Synthesis of Complex **4C**, $[Zn_2(COOEt\text{-}dfp)\ (OAc)_2](OAc)\cdot 3H_2O$.* Complex **4C** was synthesized using a procedure similar to that used for **4A**, starting from ligand **3C** (0.10 g, 0.23 mmol), $Zn(OAc)_2\cdot 2H_2O$ (0.10 g, 0.46 mmol), and TEA (0.06 mL, 0.46 mmol). The reaction product was dissolved in a methanol−chloroform (1:2, v/v) solvent mixture and kept for crystallization by slow evaporation method at room temperature. After 2 days, yellow block crystals of **4C** were obtained. Yield: 0.10 g (64%). ESI-MS: m/z 675.04 $[C_{23}H_{33}N_2O_{13}Zn_2]^+$ (calcd 675.05). Anal. Calcd for $C_{25}H_{42}N_2O_{18}Zn_2$: C, 38.04; H, 5.36; N, 3.55. Found: C, 38.03; H, 5.37; N, 3.66. IR (ATR, cm^{-1}): 3260 (O−H), 2827 (C−H), 1697 (C═O, ester), 1631 (C═N).

*Synthesis of Complex **4D**, $[Zn_2(Br\text{-}dfp)\ (OAc)_2](OAc)\cdot H_2O$.* Complex **4D** was synthesized using a procedure similar to that used for **4A**, starting from ligand **3D** (0.20 g, 0.46 mmol), $Zn(OAc)_2\cdot 2H_2O$ (0.20 g, 0.92 mmol), and TEA (0.13 mL, 0.92 mmol). The reaction product was dissolved in a methanol−chloroform (1:2) solvent mixture and kept for crystallization by diffusion with diethyl ether at room temperature. After 2 days, yellow block crystals of **4D** were obtained. Yield: 0.22 g (70%). ESI-MS: m/z 680.98 $[C_{20}H_{28}BrN_2O_{11}Zn_2]^+$ (calcd 680.94). Anal. Calcd for $C_{22}H_{35}BrN_2O_{15}Zn_2$: C, 33.95; H, 4.53; N, 3.60. Found: C, 33.63; H, 5.01; N, 3.64. IR (ATR, cm^{-1}): 3248 (O−H), 2886 (C−H), 1632 (C═N).

Procedure Employed To Dope Complexes 4A−4D into PMMA Matrix. A solution of methyl methacrylate monomer containing 0.3% (w/w) azobis(isobutyronitrile) (AIBN) initiator was heated at 75 °C. After 24 h, the required amount of Zn complex (**4A**/**4B**/**4C**/**4D**) in 20 μL of methanol was added into the resulting viscous solution of PMMA. 2−3 mL of tetrahydrofuran solvent was added and stirred again at the same temperature for 2 h. The mixture was poured into glass molds and cured at 75 °C under vacuum.[20]

Catalytic Activities of Complexes 4A−4D. *Transesterification of Phenylacetate with Various Alcoholic Substrates.* Two mL of alcoholic solution of phenyl acetate (PA) (1.0 mmol) containing 0.01 mmol (ca. 6.0 mg) of catalyst (complex **4A**/**4B**/**4C** or **4D**) was stirred in a glass tube equipped with Teflon lined screw cap at 50 °C for 20 h. After this, the reaction mixture was filtered, the filtrate was diluted with dichloromethane (DCM), and the total volume of the solution was made up to 10 mL. This solution was filtered again by using nylon-6 filter (0.22 μm) and subjected to gas chromatography (GC) as well as ESI-MS analyses. The yield of the reaction was calculated by GC using the internal standard (1,2,4-trimethylbenzene) method,[21] see the Supporting Information. All reactions were run at least three times, and the average conversion yields are reported here.

Transesterification of Triacetin with Methanol. Triacetin (0.65 mmol) was dissolved in 4 mL of methanol taken in a round-bottom flask equipped with a reflux condenser. Complex catalyst (**4A**/**4B**/**4C** or **4D**) (0.02 mmol or ca. 12 mg) was added into this solution and stirred at 50 °C for 24−26 h. After this, the reaction mixture was

DOI: 10.1021/acs.inorgchem.6b00804
Inorg. Chem. XXXX, XXX, XXX−XXX

filtered and the filtrate was made up to 10 mL using dichloromethane (DCM). This solution was filtered again by using a nylon-6 filter (0.22 μm) and analyzed by GC. The yields were calculated by GC using an internal standard (1,2,4-trimethylbenzene) method, see the Supporting Information. All reactions were run at least three times, and the average conversion yields are reported here.

Transesterification of a Vegetable Oil (Canola Oil) with Methanol. The transesterification of canola oil was carried out in a glass tube equipped with a Teflon lined screw cap. A solution of 50.0 μL of canola oil in 4 mL of methanol was used in the presence of 0.01 wt % of complex **4A**/**4B**/**4C** or **4D** as catalyst. The reaction mixtrue was stirred magnetically at 50 °C for 24−26 h. After this, the reaction mixture was transferred into a separating funnel, and 10 mL of dichloromethane/water (1:1, v/v) mixed solvent was added. The solution was shaken vigorously and allowed to settle down. After the formation of two layers, the lower organic layer was removed and washed with 5 × 10 mL of water for removing the catalyst as well as any byproduct formed. The organic phase was dried over anhydrous sodium sulfate, and the solvent was removed by rotary evaporater. The final product was dried overnight at 40 °C. The product thus obtained was dissolved in 1 mL of DCM, and a known amount of internal standard (1,2,4-trimethylbenzene) was added to it. This solution was filtered by using nylon-6 filter (0.22 μm) and subjected to quantitative GC analysis and ^{1}H NMR spectroscopy; see the Supporting Information.

RESULTS AND DISCUSSION

Synthesis and Structures. Complexes **4A**−**4D** were prepared by reacting hrls **3A**−**3D**[10] respectively with zinc acetate in 1:2 molar ratio in the presence of triethylamine (TEA), see Scheme 1. Complexes **4A**−**4D** were characterized by standard techniques including ESI-MS, elemental analysis, and single crystal XRD analyses, see the Supporting Information.

Scheme 1. Synthetic Procedure for Diverse Zn Complexes 4A−4D

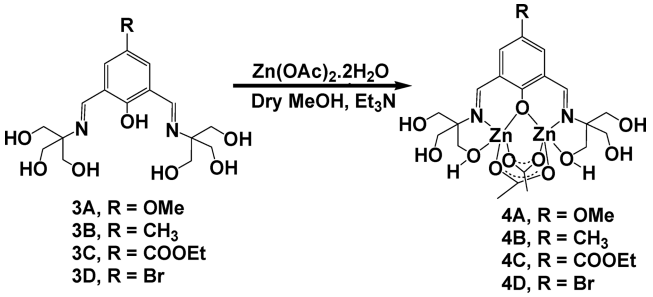

The single crystal X-ray analyses revealed that complexes **4A**−**4D** exhibit similar structural features. The structure of complex **4B** has been reported earlier.[5b] Complexes **4A** and **4D** crystallized in triclinic space group $P\bar{1}$, while complex **4C** crystallized in monoclinic space group $P2_1/c$. The crystallographic data are given in Table 1; selected bond lengths and bond angles are given in Table S1. Crystal structures of complexes **4A**, **4C**, and **4D** with atom-numbering scheme are shown in Figure 1. In these complexes, two Zn(II) centers are bridged together by phenolate oxygen of dfp ligand along with two acetate units bridging in $\mu_{1,3}$ mode. Imine nitrogen and one of the $-CH_2OH$ arms of the tris moiety coordinate to each Zn(II) center completing the square-pyramidal NO_4 coordination. Notably, the N−Zn−O(tris) bite angles are quite acute in these complexes: 79.67(9)° and 80.04(8)° for **4A**, 78.6(2)°−81.39(17)° for **4C**, and 79.95(16)° and 82.20(15)° for **4D**. The observed Zn−O distances (1.961(2)−2.157(2) Å for **4A**, 1.935(5)-2.128(4) Å for **4C**, and 1.981(4)−2.133(4) Å for **4D**) and Zn−N distances (2.019(2) and 2.027(2) Å for **4A**, 2.007(5)−2.029(4) Å for **4C**, and 2.013(4) and 2.023(4) Å for **4D**) are quite in agreement with the bond distances reported for similar complexes in the literature.[5b] The Zn−O−Zn angles are 101.99(8)° for **4A**, 100.15(16)° and 100.52(16)° for **4C**, and 101.45(14)° for **4D**. The $Zn_1\cdots Zn_2$ separations are quite comparable: 3.221 Å for **4A**, 3.193 and 3.194 Å for **4C**, and 3.198 Å for **4D**.

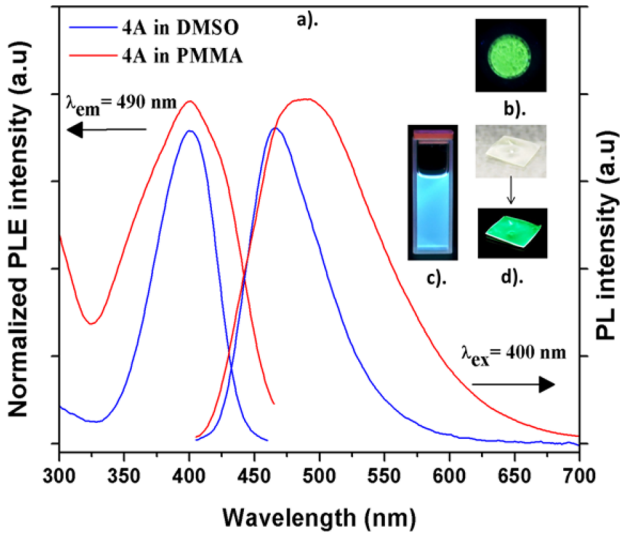

Figure 2. (a) PL excitation (PLE) and emission (PL) spectra (left and right panels, respectively) of complex **4A** in DMSO and in PMMA matrix. The PL and PLE spectra were excited and recorded at 400 and 490 nm, respectively. (b) Solid state image of **4A** in $BaSO_4$ under 365 nm irradiation. (c) **4A** in DMSO under UV irradiation (365 nm). (d) PMMA sheet containing **4A** under visible light (above) and under 365 nm irradiation (below).

Table 2. Photophysical Properties of Complexes 4A−4D

	4A	4B	4C	4D
	In DMSO Solvent			
$\lambda_{abs\text{-}sol}$ [nm][a]	410	388	352	381
λ_{em} [nm][b]	470	457	423	456
τ_{av} [ns][c]	1.93	1.37	0.38	0.24
Φ_{total}[d] [%]	27.66	15.74	10.18	9.4
	In PMMA Matrix			
$\lambda_{abs\text{-}sheet}$ [nm][e]	400	380	360	380
λ_{em} [nm][f]	490	460	422	458
τ_{av} [ns][g]	1.4	1.98	0.41	0.58
Φ_{total}[h] [%]	15.55	14.18	5.52	4.82
	In the Solid State			
Φ_{total}[i] [%]	7.41	4.94	3.64	0.59
λ_{ex} [nm][j]	400	380	360	380

[a]Wavelength of UV/visible absorbance maximum in DMSO. [b]Wavelength of emission (PL) maximum in DMSO. [c]Average lifetime of complexes in DMSO excited by 390 nm. [d]PL quantum yield (%) of complexes in DMSO. [e]Wavelength of UV/visible absorbance maximum in PMMA. [f]Wavelength of emission (PL) maximum in PMMA. [g]Average lifetime of complexes in PMMA matrix excited by 390 nm laser. [h]PL quantum yield (%) of complexes in PMMA. [i]PL quantum yield (%) of complexes in the solid state. [j]Excitation wavelength for PLQY measurement in all cases.

DOI: 10.1021/acs.inorgchem.6b00804
Inorg. Chem. XXXX, XXX, XXX−XXX

Table 3. Optical and Electrochemical Properties of Complexes 4A–4D

complexes	λ_o[a] (nm)	$E_{g,opt}$[b] (eV)	$E_{red,onset}$[c] (V)	LUMO[d] (eV)	HOMO[e] (eV)
4A	432	2.87	−1.53	−2.81	−5.68
4B	412	3.01	−1.48	−2.86	−5.87
4C	392	3.16	−1.41	−2.93	−6.09
4D	410	3.02	−1.32,	−3.02	−6.04

[a]Recorded from the intersection of absorption and emission spectra in solutions. [b]$E_{g,opt} = 1240/\lambda_o$. [c]Reduction potential vs Ag/Ag^+ in DMSO solution with 0.1 M n-Bu_4NPF_6 as supporting electrolyte, scan speed 100 mV s^{-1} ($E_{1/2,Fc/Fc^+} = 0.46$ V). [d]Calculated based on $E_{LUMO} = -(4.8 - E_{1/2,Fc/Fc^+} + E_{red,onset})$. [e]Estimated from $E_{HOMO} = E_{LUMO} - E_{g,opt}$.

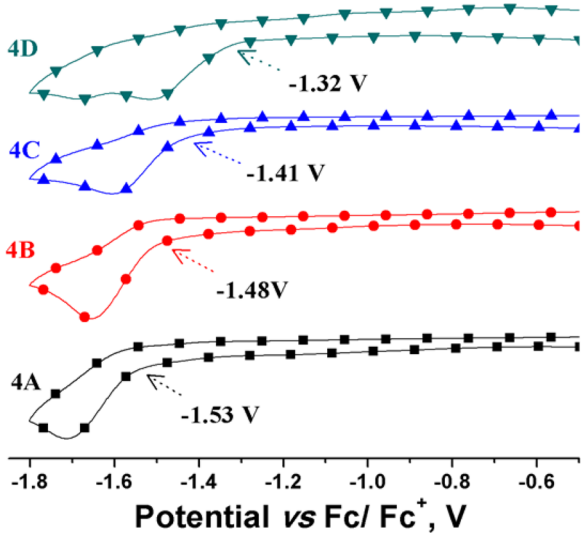

Figure 3. Cyclic voltammograms of 5×10^{-3} M solutions of **4A**, **4B**, **4C**, and **4D** in DMSO containing 0.1 M n-Bu_4NPF_6. Scan rate, 100 mVs^{-1}; working electrode, glassy carbon; reference electrode, Ag/AgCl.

Photophysical Properties. Luminescence properties of compartmental Schiff base complexes have attracted the attention of researchers working in diverse areas, but the majority of such studies have been conducted in solutions.[4] However, systems capable of exhibiting fluorescence in the solid state may find applications in optoelectronic devices. Therefore, we decided to explore the luminescent properties, lifetimes, and total quantum yields of complexes **4A–4D** in powdered form as well as in solid poly(methyl methacrylate) (PMMA) matrix in addition to studies in DMSO solutions. Representative fluorescence spectra of complex **4A** in PMMA matrix and in DMSO solution are shown in Figure 2.

Similar spectra of other complexes are given in Figures S6–S8. The relevant PL excitation (PLE) and emission (PL) spectral data are summarized in Table 2. The electronic spectra of complexes **4A–4D** showed absorptions in the range 350–410 nm. A bathochromic shift of this band was observed for

Table 4. Transesterification of Phenyl Acetate with Various Alcohols by Catalysts 4A–4D at 50 °C[a]

entry	substrate	catalyst	yield[b] (%)	product
1	benzyl alcohol	**4A**	83	benzyl acetate
		4B	46	
		4C	44	
		4D	64	
2	methanol	**4A**	100	methyl acetate[c]
		4B	52	
		4C	38	
		4D	74	
3	ethanol	**4A**	100	ethyl acetate
		4B	84	
		4C	87	
		4D	99	
4	isopropanol	**4A**	46	isopropyl acetate
		4B	31	
		4C	31	
		4D	40	
5	1-butanol	**4A**	68	butyl acetate
		4B	62	
		4C	60	
		4D	61	
6	1-hexanol	**4A**	80	hexyl acetate
		4B	77	
		4C	64	
		4D	79	

[a]Reaction conditions: phenyl acetate 1.0 mmol (127.0 mL); catalyst 0.01 mmol; 2 mL of alcohols at 50 °C for 20 h. [b]Yields based on GC analysis. [c]1.5 mmol (190.0 mL) of phenyl acetate; 0.015 mmol catalyst; 3.0 mL of alcohols at 50 °C for 20 h. Reaction was performed in a round-bottom flask equipped with reflux condenser. DB-wax column was used for methyl acetate analysis.

Table 5. Transesterification of Triacetin and Canola Oil by Catalysts 4A–4D in Methanol at 50 °C

		yields (%) or conversion (%)			
entry	substrate	**4A**	**4B**	**4C**	**4D**
1	triacetin[a]	99	37	35	78
2	canola oil[b]	5	3	2	5

[a]Methyl acetate as a product was formed after reaction of triacetin with methanol in the presence of catalysts. [b]Conversion percentage of canola oil to fatty acid methyl esters (FAME) was calculated by using GC data.

complexes having a strong electron donating group at the para position of the phenolate oxygen. The molar extinction coefficient (ε) values were in the range $(3.45 \pm 0.04) \times 10^3$ to $(8.35 \pm 0.44) \times 10^3$ for these complexes with complex **4D** having the lowest and complexes **4B** and **4C** having the highest ε values (Figures S9–S12). The complexes **4A–4D** showed fluorescence emission in solutions, in the doped state in PMMA matrix, and in the solid state at room temperature. The emission maxima of complexes **4A–4D** can mostly be

Scheme 2. Transesterification of Phenyl Acetate with Various Alcoholic Substrates (R′ = Methyl, Ethyl, Isopropyl, Butyl, Hexyl, and Benzyl) Catalyzed by Complexes 4A–4D

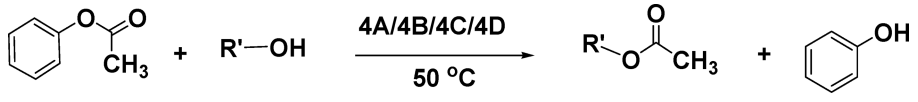

DOI: 10.1021/acs.inorgchem.6b00804
Inorg. Chem. XXXX, XXX, XXX–XXX

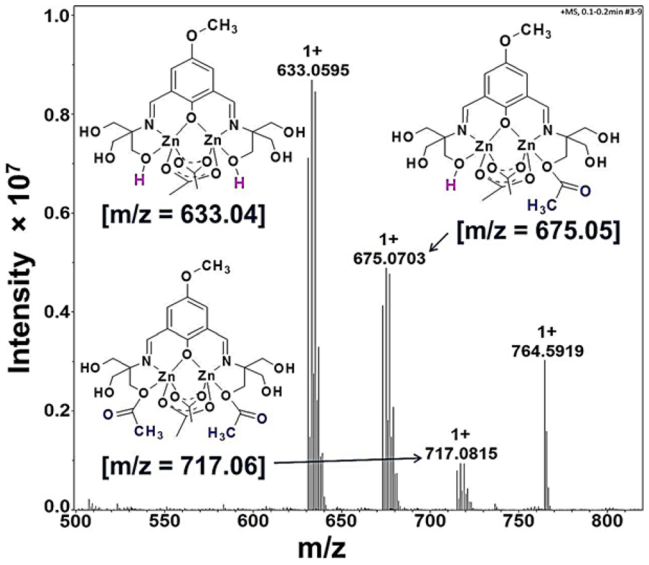

Figure 4. ESI-MS spectrum of the reaction mixture of the transesterification reaction involving PA, MeOH, and complex **4A** as catalyst showing the formation of two acyl intermediate species.

attributed to the ligand-centered transitions. The observed emission (PL) maxima of complexes **4A**, **4B**, **4C**, and **4D** in DMSO were 470, 457, 423, and 456 nm respectively with bright−blue emission. However, the corresponding emission maxima in PMMA matrix showed either a small hypsochromic shift (∼1 nm in **4C**) or a bathochromic shift (∼2−3 nm in **4B** and **4D**) (Figures S6−S8). But complex **4A** in PMMA matrix showed a broad spectrum with a large bathochromic shift of ∼20 nm with a yellowish−green emission (shown in Figure 1).

These shifts probably indicate the suppression of rotation of the para substituent by PMMA matrix and accompanied increases in the rigidity of the complex due to higher microviscosity. The nature of the excited state also gets affected by its environment (Figures S9−S10 and Table 2); such effects have been reported earlier.[22] The observed total photoluminescence quantum yields (PLQY) (Φ_{total}) of complexes **4A**−**4D** were in the range 7.41−0.59% for pure powdered samples and between 15.55 and 4.82% when doped in PMMA matrix (Table 2). The striking increase of the PLQY in the PMMA matrix could be attributed to the increase in $\pi \rightarrow \pi^*$ ILCT in comparison to that in pure powder form.[22a] The PLQY values exhibited by complexes **4A**−**4D** in PMMA matrix were strongly governed by the electronic nature of the ligand substitution. Complex **4A** gives rise to the highest Φ_{total} probably due to the efficient ILCT from −OMe group. Meanwhile, the PLQY values observed for complexes **4A**−**4D** in solutions were in the range 27.22−9.40%, which are higher than that observed in PMMA matrix. In the solution state, significant H-bonding interactions are possible between various functional groups present on the complex molecules and O═S groups of the DMSO solvent molecules, which could play significant roles in increasing the Φ_{total} values in solutions in comparison to those in PMMA matrix.[23] The fluorescence lifetimes of the complexes **4A**−**4D** in solution and in PMMA matrix were in the range 1.93−0.24 ns (Figures S13−S16, Table 2). The complexes **4A**−**4D** therefore show interesting photophysical properties in the solid state, in solutions, and in PMMA matrix. The PLQY values exhibited by **4A**−**4D** are comparable to (or greater than) those reported for similar complexes.[24] The shift observed in the emission wavelengths as a function of ligand substitution is of interest as it shows the potential of fine-tuning the fluorescent properties of this class of complexes by changing the substituents on the ligand backbone. In some cases, especially in the case of complex **4A**, the use of PMMA matrix affects the color of the emission considerably compared to that in pure solid form or in solution. Owing to their good performance as solid-state emitters, these complexes exhibit potential as tunable fluorescent candidates for optoelectronic devices.[25]

Electrochemical Properties. The electrochemical properties of complexes **4A**−**4D** were investigated by cyclic voltammetry (CV) in DMSO solutions, and the results are summarized in Table 3 and Figure 3. The CV data showed that the complexes **4A**−**4D** display irreversible reduction responses at half-wave potentials of approximately −1.71, −1.65, −1.60, and −1.51 V vs Fc/Fc^+, respectively. In the literature, similar irreversible reduction responses have been reported for Zn complexes, that are attributed to the generation of rare, unstable, and low valent Zn(I) species.[26] As the generation of Zn(I) requires an electron to enter the 4s orbital, often high potentials are required for such electron transfer.[27] To confirm the reduction site, CVs of free ligands were recorded which showed no electroactivity (Figure S17). Moreover, it is observed that the presence of electron donating substituents on ligands pushes the reduction half-wave potential to more negative values as expected (Figure 3). Giannicchi et al. have reported the shifting of reduction potential to more negative values with inductively electron donating group (EDG).[28]

In continuation, we were interested in calculating the HOMO−LUMO energy levels of complexes **4A**−**4D** for assessing their potential for optoelectronic devices. The LUMO energy levels of complexes **4A**−**4D** were calculated from the reduction onset potential values ($E_{red,onset}$).[13] The HOMO energy levels were then calculated from the respective LUMO energy level values and optical band gap values. The optical band gap values in turn were obtained from the intersection of absorption and emission spectra.[14] The optical and electrochemical properties of complexes **4A**−**4D** are summarized in Table 3. The HOMO and LUMO energy levels of Zn(II) complexes **4A**−**4D** were estimated to be in the ranges −5.68 to −6.04 eV and −2.81 to −3.02 eV respectively. Overall, the HOMO and LUMO energy levels decrease systematically on changing the ligand substituents from electron donating (−OMe/$-CH_3$) groups to electron withdrawing (−COOEt/−Br) groups. However, the LUMO energy levels were less sensitive to substituent variations compared to HOMO levels and show a variation of only ∼Δ0.2 eV.[29] These results correlate well with the blue shifts observed in the absorption (λ_{abs}) and emission (λ_{em}) wavelengths of complexes **4A**−**4D** (Table 2). The HOMO and LUMO energy level values of complexes **4A**−**4D** are comparable to those of similar Zn complexes reported for optoelectronic devices.[8b,29] Therefore, we assume that complexes **4A**−**4D** may attract attention as candidates for optoelectronic devices.

Catalytic Transesterification. Zn-alcoholic OH moieties in biological enzymes and in analogous complexes are known to play crucial roles in catalytic transformations like ester hydrolysis and transesterification.[7] We tested complexes **4A**−**4D** as catalysts for the transesterification of phenyl acetate (PA) with alcohol substrates (Scheme 2).

The reaction of PA with benzyl alcohol (BnOH) in the presence of complexes **4A**−**4D** as catalysts produced benzyl

DOI: 10.1021/acs.inorgchem.6b00804
Inorg. Chem. XXXX, XXX, XXX−XXX

Scheme 3. Plausible Mechanism for the Transesterification of PA Promoted by Complex 4A/4B/4C or 4D as Catalyst

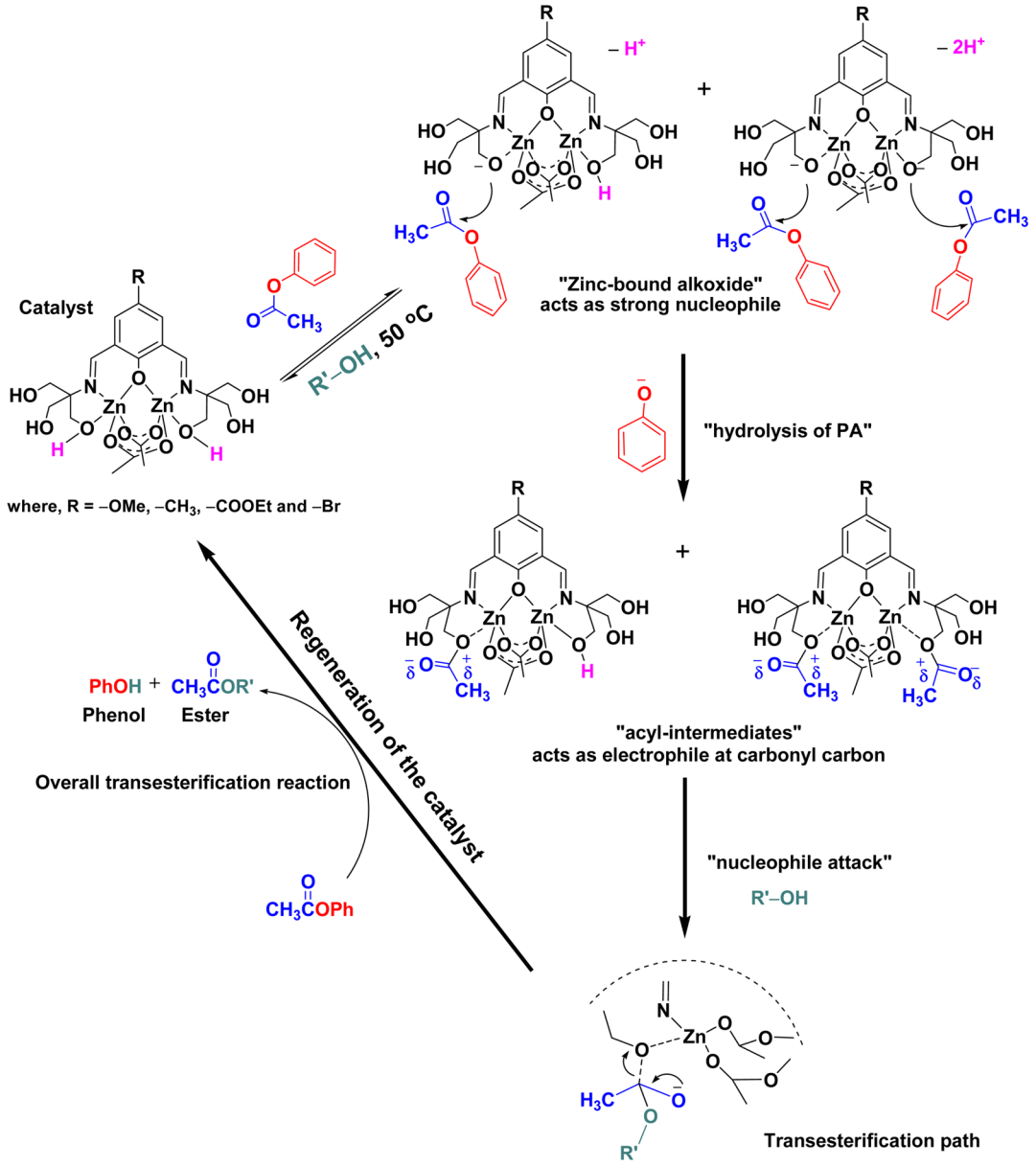

Scheme 4. Transesterification of a Vegetable Oil (Canola Oil) with Methanol Catalyzed by Complexes 4A–4D[a]

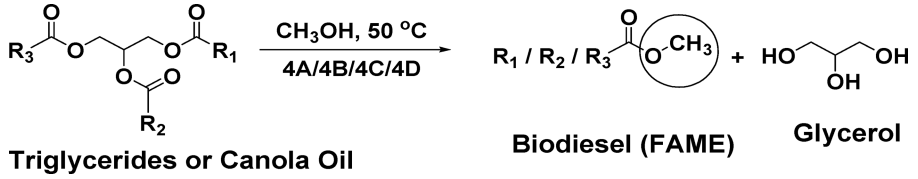

[a]Here R_1, R_2, and R_3 may be oleic (C18:1), linoleic (C18:2), and linolenic (C18:3) respectively.

acetate (BnA) quantitatively within 20 h under neutral conditions, see Scheme 2 and entry 1 of Table 4. The results obtained with complexes **4A–4D** are better than those with some of the previously reported Zn complex catalysts for BnA production, which yielded 15% in 18 h.[30]

We also tested **4A–4D** as catalysts for the transesterification of triacetin (TA), a model compound for larger triglycerides as found in vegetable oils and fats, with methanol at 50 °C (see Scheme S2). Complex **4A** successfully catalyzed the conversion of triacetin to methyl acetate with 99% yields on reaction with methanol within 24 h, while the complexes **4B**, **4C**, and **4D** catalyzed the same conversion only in moderate yields, see entry 1 of Table 5.

ESI-MS Studies To Elucidate a Plausible Mechanism for Transesterification by 4A–4D. In order to identify the various species involved in the catalytic process and hence to understand the mechanism of transesterification in detail, we conducted ESI-MS spectral analyses on model reactions

DOI: 10.1021/acs.inorgchem.6b00804
Inorg. Chem. XXXX, XXX, XXX–XXX

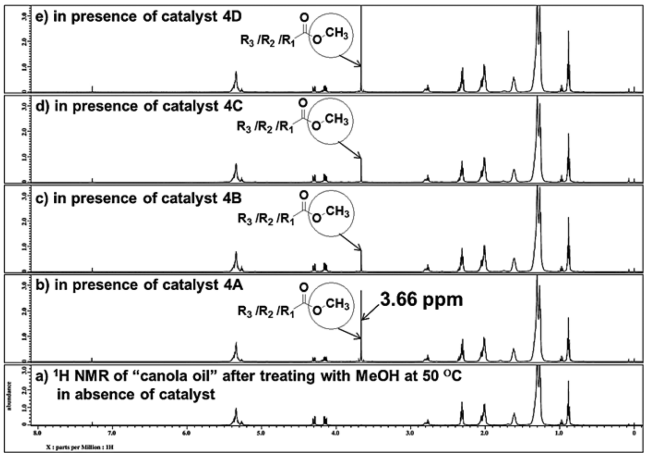

Figure 5. ^{1}H NMR spectra of canola oil after treating with MeOH at 50 °C (a) in the absence of any catalyst, (b) in the presence of complex **4A** as catalyst, (c) in the presence of complex **4B** as catalyst, (d) in the presence of complex **4C** as catalyst, and (e) in the presence of complex **4D** as catalyst.

involving complexes **4A**−**4D** as catalysts and PA as substrate in excess (catalyst/PA molar ratio = 1/100) in alcoholic solutions. These studies suggest that in every case two "acyl intermediate species" $[Zn_2(R\text{-dfp} - H)(O_2CMe)_2(CH_3CO)]^+$ and $[Zn_2(R\text{-dfp} - 2H)(O_2CMe)_2(CH_3CO)_2]^+$ were formed in the reaction mixture corresponding to the attachment of one or two CH_3CO^+ group(s) onto the alkoxide oxygen(s) of the catalyst as shown in Figure 4 and Figures S18, S19, and S20. Based on the species identified in ESI-MS, a plausible mechanism for catalysis by complexes **4A**−**4D** is proposed, see Scheme 3. Deprotonation of Zn(II) bound alcoholic OH group in similar cases has already been reported by Xia et al.[7] Zn-bound alkoxide acts as strong nucleophile for hydrolysis of PA. The attack of Zn(II)-coordinated alkoxide on the carbonyl carbon of PA in solution leads to the generation of "acyl intermediates" as shown in Scheme 3. Further, nucleophilic R′−OH attacks the "Zn-alkoxide acyl intermediate" with electrophilic carbonyl carbon regenerating the catalyst.

As per the mechanism given in Scheme 3, Zn(II)-bound alkoxides of complexes **4A**−**4D** act as strong nucleophiles activating the carbonyl center of PA for hydrolysis. However, the nucleophilic nature of Zn(II)-bound alkoxides in complexes **4A**−**4D** depends to a large extend on the electronic properties of the 4-substituent on dfp ligand. Electron donating −OMe substituent leads to increased electron density at the Zn(II) center[28] and hence increased nucleophilicity of the Zn(II)-bound alkoxide. Electron withdrawing substituents decrease the electron density at the Zn(II) center and hence decrease the nucleophilicity of Zn(II)-bound alkoxide. In −Br substituted complex, a resonance effect of the lone pair on −Br can be expected to dominate over its negative inductive effect thus increasing the electron density at the Zn(II) center in comparison to other electron withdrawing substituents.[31] Based on the above arguments, a gradual decrease in the nucleophilicity of Zn(II)-alkoxides in complexes **4A**−**4D** is expected in the order **4A** (−OMe) > **4D** (−Br) > **4B** ($-CH_3$) > **4C** (−COOEt), which correlates very well with their observed transesterification catalytic activities. Transesterification of PA with other alcohols using complexes **4A**−**4D** as catalysts was also tested, and the results are given in Table 4.

Transesterification of Canola Oil (CO) with Methanol.

In continuation, we also tested complexes **4A**−**4D** as catalysts for the transesterification of vegetable oils to their corresponding fatty acid methyl esters (FAME) toward the generation of biodiesel (Scheme 4).

Complex **4A** showed 25% conversion of canola oil to corresponding FAME within 24 h (entry 2 of Table 5) confirmed by GC (pp S32−S37) and ^{1}H NMR data (Figure 5). ^{1}H NMR showed the characteristic −OMe peak of FAME at 3.66 ppm, in accordance with similar reports in the literature (see Figure 5).[32] Other catalysts also showed similar conversion but in lower yields. The commonly used catalysts for biodiesel generation such as H_2SO_4 and NaOH (or KOH) are highly corrosive and are known to cause saponification.[33] The use of catalysts such as complexes **4A**−**4D** may therefore help to overcome such problems.

CONCLUSION

In conclusion, a series of multifunctional binuclear Zn(II) complexes **4A**−**4D** have been developed from compartmental Schiff base hrls. Complexes **4A**−**4D** demonstrated medium-to-high PL efficiency in solutions and in PMMA matrix. Considerable dependence of the emission wavelength on the electronic nature of the ligand substitution was observed for these complexes revealing their potential as tunable materials for optoelectronic devices. In addition, complexes **4A**−**4D** act as catalysts for transesterification with complex **4A** having an −OMe substituent on the ligand backbone exhibiting maximum efficiency. Complex **4A** also catalyzed the transesterification of canola oil revealing its potential in biodiesel generation from vegetable oil. Mechanistic investigations using ESI-MS studies revealed that the transesterification by complexes **4A**−**4D** proceeds through acyl intermediates. The photoluminescence and catalytic properties exhibited by complexes **4A**−**4D** can mainly be attributed to their different structural subunits: aromatic-diimine motif and Zn-alcoholic OH units, respectively.

ASSOCIATED CONTENT

Supporting Information

The Supporting Information is available free of charge on the ACS Publications website at DOI: 10.1021/acs.inorgchem.6b00804.

Detailed characterization, photophysical, electrochemical, and GC data (PDF)

Crystallographic data for **4A** (CIF)

Crystallographic data for **4C** (CIF)

Crystallographic data for **4D** (CIF)

AUTHOR INFORMATION

Corresponding Author

*E-mail: pradeep@iitmandi.ac.in. Fax: (+91) 1905 267 009.

Notes

The authors declare no competing financial interest.

ACKNOWLEDGMENTS

C.P.P. thanks IIT Mandi for infrastructural facilities (AMRC) as well as financial support through Seed Grant. A.K.G. thanks MHRD, Government of India, for a fellowship.

DOI: 10.1021/acs.inorgchem.6b00804
Inorg. Chem. XXXX, XXX, XXX−XXX

REFERENCES

(1) Ma, D. L.; He, H. Z.; Leung, K. H.; Chan, D. S. H.; Leung, C. H. *Angew. Chem., Int. Ed.* **2013**, *52*, 7666.

(2) (a) Cunha-Silva, L.; Lima, S.; Ananias, D.; Silva, P.; Mafra, L.; Carlos, L. D.; Pillinger, M.; Valente, A. A.; Paz, F. A. A.; Rocha, J. *J. Mater. Chem.* **2009**, *19*, 2618. (b) Chen, P. C.; Ma, J. Y.; Chen, L. Y.; Lin, G. L.; Shih, C. C.; Lin, T. Y.; Chang, H. T. *Nanoscale* **2014**, *6*, 3503. (c) Lee, H.; Noh, T. H.; Jung, O. S. *Dalton Trans.* **2014**, *43*, 3842.

(3) Ricciardi, L.; Martini, M.; Tillement, O.; Sancey, L.; Perriat, P.; Ghedini, M.; Szerb, E. I.; Yadav, Y. J.; Deda, M. L. *J. Photochem. Photobiol., B* **2014**, *140*, 396.

(4) Andruh, M. *Chem. Commun.* **2011**, *47*, 3025.

(5) (a) Kessissoglou, D. P.; Li, X.; Butler, W. M.; Pecoraro, V. L. *Inorg. Chem.* **1987**, *26*, 2487. (b) Chandrasekhar, V.; Das, S.; Yadav, R.; Hossain, S.; Parihar, R.; Subramaniam, G.; Sen, P. *Inorg. Chem.* **2012**, *51*, 8664.

(6) Arora, H.; Barman, S. K.; Lloret, F.; Mukherjee, R. *Inorg. Chem.* **2012**, *51*, 5539.

(7) (a) Xia, J.; Shi, Y.; Zhang, Y.; Miao, Q.; Tang, W. *Inorg. Chem.* **2003**, *42*, 70. (b) Xia, J.; Xu, Y.; Li, S.; Sun, W.; Yu, K.; Tang, W. *Inorg. Chem.* **2001**, *40*, 2394. (c) Dey, M.; Rao, C. P.; Saarenketo, P.; Rissanen, K.; Kolehmainen, E. *Eur. J. Inorg. Chem.* **2002**, *2002*, 2207.

(8) (a) Petrova, P. K.; Tomova, R. L.; Stoycheva-Topalova, R. T. *Organic Light Emitting Diode- Material, Process and Devices*; Ko, S. H., Ed.; InTech: 2011; Chapter 6. (b) Xu, H.; Chen, R.; Sun, Q.; Lai, W.; Su, Q.; Huang, W.; Liu, X. *Chem. Soc. Rev.* **2014**, *43*, 3259. (c) Dumur, F. *Synth. Met.* **2014**, *195*, 241.

(9) Lee, A. F.; Bennett, J. A.; Manayil, J. C.; Wilson, K. *Chem. Soc. Rev.* **2014**, *43*, 7887.

(10) Gupta, A. K.; Dhir, A.; Pradeep, C. P. *Eur. J. Org. Chem.* **2015**, *2015*, 122.

(11) Brouwer, A. M. *Pure Appl. Chem.* **2011**, *83*, 2213.

(12) (a) Liu, Y.; Liu, M. S.; Jen, A. K. -Y. *Acta Polym.* **1999**, *50*, 105. (b) Li, Y.; Cao, Y.; Gao, J.; Wang, D.; Yu, G.; Heeger, A. J. *Synth. Met.* **1999**, *99*, 243.

(13) (a) Tsai, J.-H.; Lee, W.-Y.; Chen, W.-C.; Yu, C.-Y.; Hwang, G.-W.; Ting, C. *Chem. Mater.* **2010**, *22*, 3290. (b) Lu, C.; Wu, H. C.; Chiu, Y. C.; Lee, W. Y.; Chen, W. C. *Macromolecules* **2012**, *45*, 3047.

(14) Kumar, S.; Thomas, K. R. J.; Li, C.-T.; Ho, K.-C. *Org. Electron.* **2015**, *26*, 109.

(15) *CrysAlisPro Program, version171.37.33c*; Agilent Technologies: Oxford, 2012.

(16) Sheldrick, G. M. *Acta Crystallogr., Sect. A: Found. Crystallogr.* **2008**, *A64*, 112.

(17) Dolomanov, O. V.; Bourhis, L. J.; Gildea, R. J.; Howard, J. A. K.; Puschmann, H. J. *J. Appl. Crystallogr.* **2009**, *42*, 339.

(18) Spek, A. L. *Acta Crystallogr., Sect. D: Biol. Crystallogr.* **2009**, *D65*, 148.

(19) Arafa, W. A. A.; Kärkäs, M. D.; Lee, B. L.; Åkermark, T.; Liao, R. Z.; Berends, H. M.; Messinger, J.; Siegbahn, P. E. M; Åkermark, B. *Phys. Chem. Chem. Phys.* **2014**, *16*, 11950.

(20) Moudam, O.; Rowan, B. C.; Alamiry, M.; Richardson, P.; Richards, B. S.; Jones, A. C.; Robertson, N. *Chem. Commun.* **2009**, 6649.

(21) Pradeep, C. P.; Htwe, T.; Zacharias, P. S.; Das, S. K. *New J. Chem.* **2004**, *28*, 735.

(22) (a) Zehnder, T. N.; Blacque, O.; Venkatesan, K. *Dalton Trans.* **2014**, *43*, 11959. (b) Moudam, O.; Rowan, B. C.; Alamiry, M.; Richardson, P.; Richards, B. S.; Jones, A. C.; Robertson, N. *Chem. Commun.* **2009**, 6649.

(23) Mukhopadhyay, M.; Banerjee, D.; Mukherjee, S. *J. Phys. Chem. A* **2006**, *110*, 12743.

(24) Hickey, J. L.; James, J. L.; Henderson, C. A.; Price, K. A.; Mot, A. I.; Buncic, G.; Crouch, P. J.; White, J. M.; White, A. R.; Smith, T. A.; Donnelly, P. S. *Inorg. Chem.* **2015**, *54*, 9556.

(25) Anthony, S. P. *ChemPlusChem* **2012**, *77*, 518.

(26) (a) Mazaletskii, A. B.; Zverev, A. N.; Vinogradova, V. G.; Alam, L. V.; Kvitko, I. Y. *Zh. Obshch. Khim.* **1991**, *61*, 2215. (b) Cox, H.; Norris, C.; Wu, G.; Guan, J.; Hessey, S.; Stace, A. J. *Dalton Trans.* **2011**, *40*, 11200. (c) Bollermann, T.; Gemel, C.; Fischer, R. A. *Coord. Chem. Rev.* **2012**, *256*, 537.

(27) Donovan, E. S.; Barry, B. M.; Larsen, C. A.; Wirtz, M. N.; Geiger, W. E.; Kemp, R. A. *Chem. Commun.* **2016**, *52*, 1685.

(28) Giannicchi, I.; Brissos, R.; Ramos, D.; Lapuente, J. d.; Lima, J. C.; Cort, A. D.; Rodríguez, L. *Inorg. Chem.* **2013**, *52*, 9245.

(29) (a) Son, H.-J.; Han, W.-S.; Chun, J.-Y.; Kang, B.-K.; Kwon, S.-N.; Ko, J.; Han, S. J.; Lee, C.; Kim, S. J.; Kang, S. O. *Inorg. Chem.* **2008**, *47*, 5666. (b) Li, Z.; Dellali, A.; Malik, J.; Motevalli, M.; Nix, R. M.; Olukoya, T.; Peng, Y.; Ye, H.; Gillin, W. P.; Hernández, I.; Wyatt, P. B. *Inorg. Chem.* **2013**, *52*, 1379.

(30) Zhang, G.; Jia, Y. X.; Chen, W.; Lo, W. F.; Brathwaite, N.; Golen, J. A.; Rheingold, A. L. *RSC Adv.* **2015**, *5*, 15870.

(31) (a) Dochnahl, M.; Löhnwitz, K.; Lühl, A.; Pissarek, J.-W.; Biyikal, M.; Roesky, P. W.; Blechert, S. *Organometallics* **2010**, *29*, 2637. (b) Duan, R.; Gao, B.; Li, X.; Pang, X.; Wang, X.; Shao, H.; Chen, X. *Polymer* **2015**, *71*, 1. (c) Yam, V. W. -W.; Pui, Y.-L.; Cheung, K.-K. *Inorg. Chem.* **2000**, *39*, 5741.

(32) Moser, B. R.; Knothe, G.; Cermak, S. C. *Energy Environ. Sci.* **2010**, *3*, 318.

(33) Ataya, F.; Dubé, M. A.; Ternan, M. *Energy Fuels* **2007**, *21*, 2450.

DOI: 10.1021/acs.inorgchem.6b00804
Inorg. Chem. XXXX, XXX, XXX−XXX